Biochimica et Biophysica Acta 1838 (2014) 1862–1870

Contents lists available at ScienceDirect

Biochimica et Biophysica Acta

journal homepage: www.elsevier.com/locate/bbamem

Heterologous overexpression of a monotopic glucosyltransferase (MGS) induces fatty acid remodeling in *Escherichia coli* membranes

Candan Ariöz [a,*], Hansjörg Götzke [a], Ljubica Lindholm [a], Jonny Eriksson [b], Katarina Edwards [b], Daniel O. Daley [a], Andreas Barth [a], Åke Wieslander [a]

[a] The Arrhenius Laboratories for Natural Sciences, Department of Biochemistry and Biophysics, Stockholm University, SE-106 91 Stockholm, Sweden
[b] BMC, Department of Chemistry, Uppsala University, SE-751 23 Uppsala, Sweden

ARTICLE INFO

Article history:
Received 27 January 2014
Received in revised form 27 March 2014
Accepted 2 April 2014
Available online 12 April 2014

Keywords:
Lipid–protein interaction
Fatty acid modeling
Cyclopropanation
Membrane fluidity
Monotopic membrane protein
Intracellular membrane

ABSTRACT

The membrane protein monoglucosyldiacylglycerol synthase (MGS) from *Acholeplasma laidlawii* is responsible for the creation of intracellular membranes when overexpressed in *Escherichia coli* (*E. coli*). The present study investigates time dependent changes in composition and properties of *E. coli* membranes during 22 h of MGS induction. The lipid/protein ratio increased by 38% in MGS-expressing cells compared to control cells. Time-dependent screening of lipids during this period indicated differences in fatty acid modeling. (1) Unsaturation levels remained constant for MGS cells (~62%) but significantly decreased in control cells (from 61% to 36%). (2) Cyclopropanated fatty acid content was lower in MGS producing cells while control cells had an increased cyclopropanation activity. Among all lipids, phosphatidylethanolamine (PE) was detected to be the most affected species in terms of cyclopropanation. Higher levels of unsaturation, lowered cyclopropanation levels and decreased transcription of the gene for cyclopropane fatty acid synthase (CFA) all indicate the tendency of the MGS protein to force *E. coli* membranes to alter its usual fatty acid composition.

1. Introduction

Establishing a stable cell membrane is known to be essential for the regulation of most channels and transporters [1–4]. The stability and permeability of bacterial membranes are regulated by altering the chemical properties of membrane lipids, thus enabling the organism to adapt to changes in the extracellular milieu [5,6]. Fatty acids of lipids can easily be modified after their synthesis in a process known as *homoviscous adaptation* [7–9], which allows the cells to maintain an optimum fluidity (or viscosity) where a stable and highly selective cellular membrane can be created [10–12]. Various strategies exist for these modifications in different types of bacteria [13,14], such as (i) variation in acyl chain length distribution and (ii) introduction of branches via the β-ketoacyl-acyl carrier protein synthase III (FabH) controlled elongation pathway [9], (iii) incorporation of double bonds (unsaturation/desaturation) [14] and (iv) cyclopropanation of fatty acids [13].

Incorporation of double bonds creates a pronounced kink in the acyl chains of lipids and therefore tends to induce a disorder when all lipids are aligned in a bilayer. Thus, membranes with high unsaturated fatty acid (UFA) content have lower transition temperatures and a higher permeability compared to membranes with high saturated fatty acid (SFA) content [7,15]. Another type of modification is the conversion of a pre-existing double bonds (C═C) into their cyclic forms of methylated fatty acids (referred as *cyclopropanation*) [7,16]. This transformation is usually observed in bacteria entering the stationary phase of growth and is catalyzed by a membrane-associated enzyme called the cyclopropane fatty acid synthase (CFA), which is transcribed by the *cfa* gene [7,17]. In comparison with unsaturated fatty acids, cyclopropanated fatty acids create membranes with even lower phase-transition temperatures, increased fluidity and higher permeability to solutes (less ordered membranes) [7]. The modifications described above occur during cellular growth in order to maintain a stable and a highly selective cellular membrane.

Lipid and fatty acid modifications have been well-studied in the Gram-negative bacterium, *Escherichia coli* (*E. coli*) [18–20]. Under physiological conditions, *E. coli* has a mixture of acyl chains linked to a glycerol backbone, one saturated at the sn-1 position and the other unsaturated at the sn-2 position [21]. It can modify these fatty acids under various stress conditions [9,22–25] Changes in the saturated/unsaturated fatty acid ratio affect the fatty acid ordering of the membrane and have

Abbreviations: MGS, monoglucosyldiacylglycerol synthase; PE, phosphatidylethanolamine; PG, phosphatidylglycerol; CL, cardiolipin; GlcDAG, α-monoglucosyldiacylglycerol; CFAs, cyclopropanated fatty acids; UFAs, unsaturated fatty acids; SFAs, saturated fatty acids; CFA, cyclopropane fatty acid synthase; FAME, fatty acid methyl ester; RpoE, RNA polymerase subunit sigma 24 (σE) factor; PlsB, glycerol-3-phosphate acyltransferase; PSD, phosphatidylserine decarboxylase; FabH, β-ketoacyl-acyl carrier protein synthase; IM, inner membrane; OM, outer membrane, FT-IR, Fourier transform infrared spectroscopy; Cryo-TEM, cryo-transmission electron microscopy; FCM, flow cytometry; FSC-H, forward scatter (cell size); SSC-H, side scatter (granularity)

* Corresponding author. Tel.: +46 8 162487; fax: +46 8 153679.
E-mail address: candan@dbb.su.se (C. Ariöz).

http://dx.doi.org/10.1016/j.bbamem.2014.04.001
0005-2736/

an influence on the mobility of membrane proteins [26,27]. Motional freedom of membrane proteins in a bilayer can also be affected both by the lipid/protein ratio and the type of proteins present in the membrane [26,28,29].

Excessive production of a membrane protein is considered as a stressful condition for the cell [30,31], but it does not normally affect the intricate lipid–protein balance, since it is usually accompanied by an upregulated phospholipid synthesis so that the lipid/protein ratio remains constant [32,33]. However, some external or internal stress conditions, for example overexpression of a membrane protein affecting lipid metabolism can disturb this balance [9,34], as also found in this work. The unbalanced lipid and protein production might lead to the formation of intracellular membranes (sacks, vesicles or tubules etc.) [35–38]. A monotopic membrane protein, monoglucosyldiacylglycerol synthase (MGS) from *Acholeplasma laidlawii* was reported to result in the formation of such intracellular vesicles in *E. coli* when overexpressed [39]. Moreover, MGS overexpression has been previously shown to result in an upregulated phospholipid synthesis [40] but its connection to *homoviscous adaptation* and effects on the membrane order in *E. coli* has never been investigated previously.

Vesicle formation is an interesting but still not well-understood process. Thus understanding how MGS influences the bilayer during its induction can perhaps help us to gain further insight into the vesiculation phenomenon. Since the MGS protein is membrane-associated [41,42] and has the ability to stimulate phospholipid synthesis [40], it might also have the ability to affect fatty acid metabolism and its regulation on the packing properties of membranes. However, this possibility has not been investigated so far. We therefore investigated how *E. coli* membranes change during the induction/expression of the MGS protein by monitoring changes in lipid composition, fatty acid species and the protein/lipid ratio. Comparisons with data from investigations of regular *E. coli* membranes revealed several interesting types of modifications in membranes where the MGS protein was overexpressed. Here we report that MGS has a dramatic influence on the regulation of fatty acid synthesis, which in turn results in an alternative path for achieving membrane homeostasis.

2. Materials and methods

2.1. Growth and overexpression

The original gene for MGS protein from *A. laidlawii* was cloned into an *E. coli* strain BL21-AI™ (Invitrogen) as described previously [39,40]. During all assays BL21-AI *E. coli* strain with an empty vector served as a negative control. All transformants were selected with 100 μg/ml carbenicillin.

An overnight culture was prepared in 2× Luria–Bertani Broth (2× LB; 20 g/l Tryptone, 10 g/l yeast extract, 10 g/l NaCl) medium supplemented with 100 μg/ml carbenicillin and grown at 37 °C with 200 rpm for 15–16 h. On the next day, the overnight culture was inoculated as 1% into 2× LB fresh medium in the presence of 100 μg/ml carbenicillin. Cultures were grown at 37 °C with 200 rpm shaking until $OD_{600\ nm}$ values ~0.3–0.4 were obtained, then the temperature was decreased to 22 °C and gene expression was induced with 0.2% (w/v) L-arabinose and 1 mM isopropyl-β-D-1-thiogalactopyranoside (IPTG). Control (BL21 AI) cells not containing the MGS gene were treated equally in parallel to the cells containing the MGS gene (BL21 AI-MGS).

Vesiculation was monitored at different time points (0, 0.25, 0.5, 1, 2, 3, 4, 5, 6, 7, 8, 10 and 22 h after IPTG addition) by sampling from cultures or completely harvesting cells (if indicated).

2.2. Cryogenic transmission electron microscopy (cryo-TEM)

Cell cultures (1 ml for each time point) were harvested (13,000 rpm/4 °C/10 min.) at different time points and flash frozen in 1× phosphate-buffered saline (PBS) buffer until they were investigated by cryo-TEM [39]. The cryo-TEM measurements [43] were carried out using a Zeiss Libra 120 Transmission Electron Microscope (Carl Zeiss NTS, Oberkochen, Germany). Analysis was performed under cryo-conditions and the microscope was operating at 80 kV and in zero loss bright-field mode. Digital images were recorded under low dose conditions with a BioVision Pro-SM Slow Scan CCD camera (Proscan GmbH, Scheuring, Germany) and iTEM software (Olympus Soft Imaging System, GmbH, Münster, Germany). In order to visualize as many details as possible, an underfocus of approximately 2 μm was used to enhance the image contrast.

Prior to imaging, the samples were treated by means of placing a drop of the sample solution on a grid with a holey polymer film (hole size ~2–6 μm) and then thinned by blotting it with some filter paper. This was done in an environmental chamber at 25 °C and close to 100% humidity in order to avoid dehydration of the sample. Once blotted the sample was quickly vitrified in liquid ethane held at a temperature just above its freezing point (−183 °C). After vitrification the sample was transferred to the microscope while maintaining it cold with liquid nitrogen and avoiding air to get in contact with the sample.

2.3. Flow cytometry (FCM) analysis

Vesiculation was screened using cells (500 μl culture) harvested at different stages of induction. Pelleted cells were resuspended in 500 μl BD FACS Flow™ buffer (BD Biosciences) and further diluted ×20 times. Cell membranes were stained with 1 μM FM® 4–64 membrane stain (Molecular Probes) and incubated on ice for 30 min at dark. During the flow cytometry analysis no gating was performed and 15 event/s were attained. Each run was made with 10,000 total events for each sample and the Cell Quest software was used during all measurements. Graphs were prepared with the FlowJo (Version 10.0.6) analysis software (Figure S2, Supporting Information).

2.4. Western blot analysis

Cell cultures (1 ml) were harvested as described above and were solubilised with 1 ml solubilisation buffer (100 mM HEPES, 20 mM $MgCl_2$ and 1% DDM). Samples were clarified by centrifugation at 13,000 rpm, 4 °C for 10 min. Western blots were performed with 20 μl of the clarified supernatants and proteins were detected with Penta-His™ antibody (BSA-free, QIAGEN) and Goat anti-mouse IgG HRP conjugate. The blots were visualized with ECLPlus Western Blotting Detection kit (GE-Healthcare) and recorded with CCD camera. Quantification of bands was performed with ImageGauge 4.0 software (FujiFilm Science Lab). A calibrated western blotting was performed to calculate the number of MGS molecules per cell for each time point. A purified MGS sample was applied in parallel as a standard and developed together with MGS-induction series on the same blot and all band intensities were normalized against previously measured OD_{600} values.

2.5. Lipid extraction and thin-layer chromatography (TLC)

Radioactive lipid analysis was performed with cell cultures (10 ml) grown as described previously. 0.1 μCi/ml of [1-^{14}C] acetate (Perkin Elmer, 55.3 mCi/mmole) was included in the growth media in order to obtain fatty acid labeling. Cells were harvested completely by centrifugation at 13,000 rpm at 4 °C for 20 min. Pellets were washed with 100 mM HEPES (pH 8) buffer and frozen at −20 °C overnight. Lipids were extracted from harvested cell pellets using the Bligh & Dyer extraction protocol [44] and samples were applied onto standard Silica gel 60 TLC plates (Merck), which was then developed in a chloroform/methanol/acetic acid 85:25:10 (v/v) solvent system in one dimension. TLC plates were dried after the run at room temperature and incubated with a PhosphoImager (FujiFilm) screen for 20 h; lipid bands were then visualized and quantified by electronic autoradiography (FLA3000) using

ImageGauge 4.0 software (FujiFilm Science Lab). All TLC responses were calibrated by previously recorded OD_{600} values.

2.6. Fourier Transform Infrared Spectroscopy (FT-IR)

In order to monitor the changes in $-CH_2$ and $-CH_3$ vibrations of fatty acids, freshly collected cell pellets were analyzed with FT-IR Spectroscopy using attenuated total reflection (ATR) IR spectroscopy [45] connected to a BRUKER VERTEX 70 spectrometer equipped with a HgCdTe detector. Background spectra were taken at 20 °C against a clean empty diamond ATR crystal. 5 μl cell suspension was applied onto a diamond ATR crystal at 20 °C and samples were dried under gentle N_2 flow. Each sample measurement was repeated 15 times with a delay time of 60 s between measurements. 150 scans were run at a resolution of 4 cm^{-1} for each sample spectrum and 500 scans were run at a resolution of 4 cm^{-1} for the background measurement. The spectra were analyzed with the OPUS Spectroscopy Software (Bruker Optics). Band shifts at ~2850 cm^{-1} and ~2920 cm^{-1} that are characteristic for $-CH_2$ and $-CH_3$ vibrations were screened during induction and plotted against induction time.

Furthermore, changes in lipid/protein ratios at different time points were also screened by a calibrated IR analysis using BSA protein as a standard and *E. coli* total lipid extract (Figure S3, Supporting Information). 100 μg of BSA was applied onto the ATR crystal and increasing amounts of *E. coli* total lipid extract were mounted on top of BSA protein film (Figure S3A, Supporting Information). In each step a spectrum is taken and bands near ~1654 cm^{-1} corresponding to the amide I vibrations of proteins, ~1740 cm^{-1} corresponding to υ(C═O) vibrations of lipids were integrated separately for each spectrum. A calibration curve with high linearity ($R^2 \geq 0.9485$) was obtained using this data (Figure S3B, Supporting Information). The lipid/protein ratios for BL21 AI and BL21 AI-MGS cells were calculated from the integrations of amide I and C═O bands from the spectra taken with intact cells using this calibration curve.

2.7. Fatty acid analysis

Total lipid extracts were prepared from 200 ml cell cultures of BL21-AI and BL21-AI + MGS cells grown as described previously. Using half of the lipid extract, PE lipid was separated from other lipids (PG, CL and GlcDAG in BL21 AI-MGS clone) by preparative TLC using chloroform/methanol/acetic acid 85:25:10 (v/v/v) system and regained by scraping only the PE spot on the TLC plate. The PE lipid was reextracted from the scrapings with chloroform:methanol 2:1 (v/v) and silica particles were removed by filtering the mixture through a filter paper grade 00H (Munktell). Residual filtrate contained purified PE lipid and was concentrated under N_2 flow prior to methylation.

Methylation of PE and the rest of the total lipid extract was achieved by an overnight incubation (at 50 °C) of lipid extracts with 2% H_2SO_4 in methanol under efflux. Fatty acid methyl esters (FAMEs) were extracted with a hexane: $NaHCO_3$: Na_2SO_4 5:1:2 (v/v/v) mixture and hexane phases were collected, dried completely under N_2 flow. FAMEs were then redissolved in 200 μl hexane and kept at −20 °C until analysis. An Elite-5 (non polar) 5% diphenyl − 95% dimethylpolysiloxane 30 m × 0.25 mm × 0.25 μm GC column was equilibrated with hexane and calibrated with 1 mg/ml bacterial FAME standard mixture (Larodan). Samples were run in parallel to the standards in Perkin Elmer Clarus 400 GC system. The injection volume was 1 μl and the column temperature was kept constant at 250 °C during analysis. Triplicate measurements were performed for each sample.

2.8. Promoter activity assay for stress responses

In order to screen various stress signals during MGS induction, promoter activity reporter plasmids (*rpoE*, *cfa*, *plsB* and psD) encoding stress proteins were selected from the *E. coli* Promoter Collection (Thermo Scientific) and introduced into *E. coli* BL21-AI and *E. coli* BL21-AI + MGS cells. BL21-AI transformants were selected on LB agar supplemented with 25 μg/ml kanamycin and BL21-AI + MGS variants with 25 μg/ml kanamycin + 100 μg/ml carbenicillin. Three colonies for each transformants were grown and MGS production was induced as described above. GFP fluorescence measurements were performed as described previously [40].

3. Results

3.1. Vesiculation during MGS induction

We have previously proposed that overproduction of MGS in *E. coli* crowds the inner membrane (since the area is not adequate to insert 220,000 MGS molecules/cell) and causes membrane deformations/vesicles [39]. To determine how MGS overexpression affects membranes, we monitored BL21 AI (control) and BL21 AI-MGS (MGS-producing cells) during an induction period of 22 h (Fig. 1).

Electron microscopy (Fig. 2A and Figure S1, Supporting Information) indicated that vesicles form at very early stages of MGS induction (earlier than 1 h). A rough calculation from a calibrated western blot (Fig. 3A) indicated that only 3–4 × 10^4 MGS molecules were present in the cell at this point (data not shown). The diversity of vesicle sizes was vast but the size-distribution was predominated by vesicles with an average diameter of ≈150–200 nm (Fig. 2) as determined by visual inspection of the electron microscopy images.

Vesicle production was also monitored by a Flow Cytometer using side-scatter (SSC-H) measurements in which the cytoplasmic density of a single cell was quantitatively measured by the intensity of the light-scattered (Figure S2, Supporting Information). An increasing amount of light scattered by cells (SSC-H plots) and an unchanged cell-size (Forward scatter, FSC-H plots) indicated a progressive congestion of the cytoplasm with vesicles during MGS induction validating cryo-TEM results of the present study (Fig. 2).

3.2. Effects of MGS overexpression on membrane lipids

The lipid/protein ratio is a sensitive measure how tightly membranes are packed and can report about the order of bacterial membranes

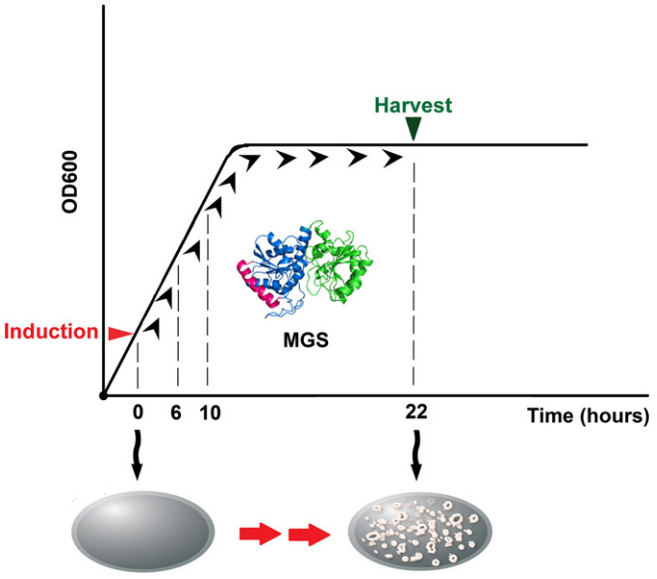

Fig. 1. A schematic representation of the experimental setup. 0 h (initiation) is the induction point where OD_{600} reaches to 0.3–0.4 and 22 h is the termination point (harvest) of the induction process. The study monitors the induction period marked with arrows. Blue and green colors on MGS structure represent N-domain and C-domain, respectively. The amphipathic binding helix (S65-L87) of MGS is shown with magenta color[40].

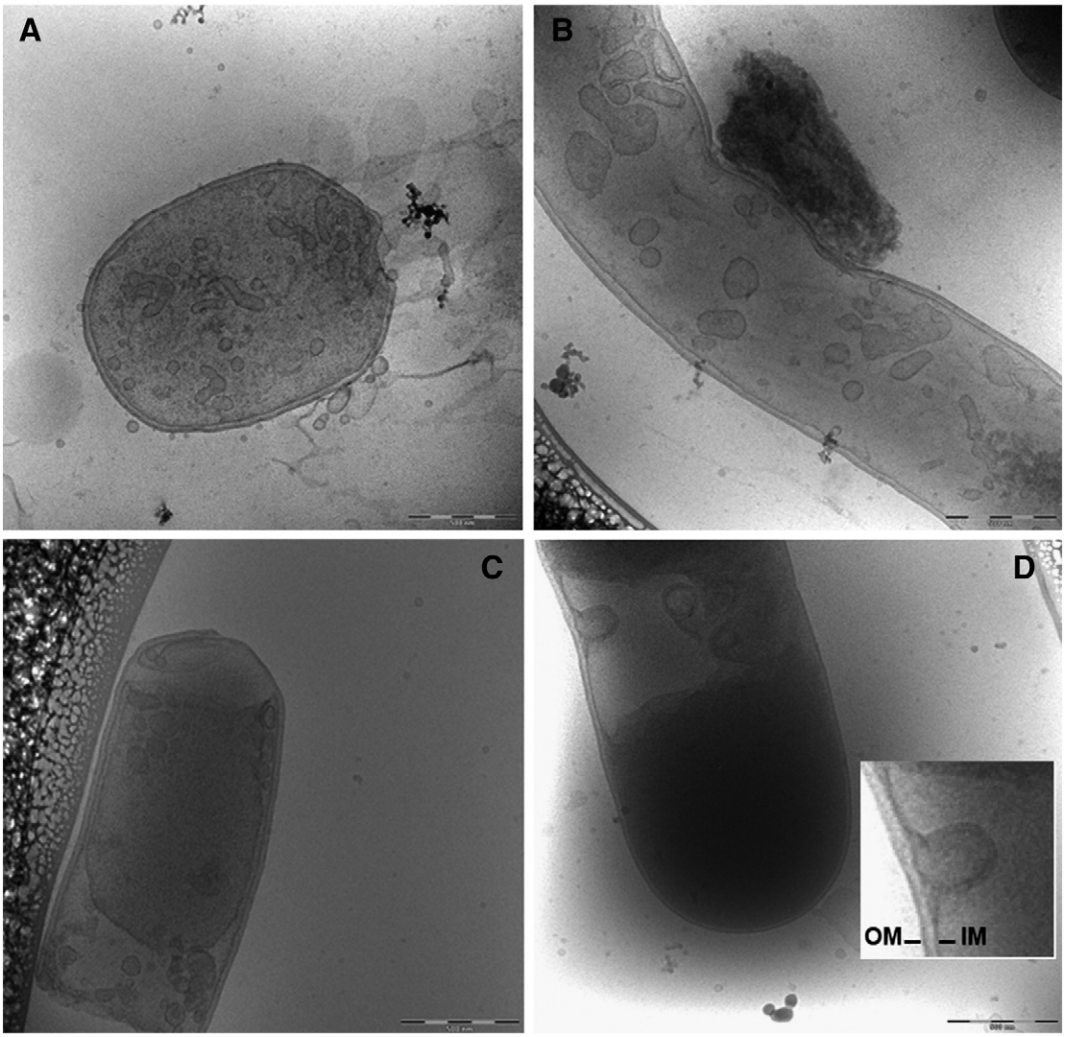

Fig. 2. Cryo-TEM pictures of *E. coli* cells overexpressing MGS protein at (A) 1 h, (B) 6 h, and (C) 22 h after induction (harvest time). (D) The convolutions of inner membrane leading to intracellular vesicles (at 22 h). IM: inner membrane, OM: outer membrane. Bars indicate 500 nm in scale.

[26,46–48]. Therefore, lipid/protein ratios of cells harvested at 0, 6 and 22 h of induction were monitored by FT-IR spectroscopy (Table 1).

No prominent change was observed in the lipid/protein ratios of BL21 AI membranes. In contrast, the lipid/protein ratio increased from 0.030 ± 0.002 to 0.040 ± 0.003 in BL21 AI-MGS cells during induction and was higher than that of the control cells after 22 h of induction (Table 1). A higher lipid/protein ratio for BL21 AI-MGS cells was also observed when plasma membrane (IM&OM) fractions (at 22 h) were compared (Table S1, Supporting Information). For the BL21 AI-MGS cells, this ratio was very similar for plasma membrane (0.048 ± 0.001) and vesicles (0.047 ± 0.002). Note that the obtained ratios were higher for membrane fractions (Table S1) than intact cells (Table 1) because of the absence of cytosolic proteins in the former samples.

To investigate this further, we monitored lipid production by thin layer chromatography (TLC) (Fig. 3). Progressive MGS production within the cell (Fig. 3A) led to a stepwise-increase in lipid synthesis (Fig. 3C). Lipid/protein ratios calculated from western and TLC responses per cell were in good correlation with lipid/protein ratios of infrared measurements (data not shown).

Thin layer chromatography (TLC) can detect differences in polarity caused by differences in molecular structures. Therefore any gradual modification on lipids can easily be monitored by the migration profiles of lipids on a TLC plate. Migration profiles of BL21 AI-MGS lipids (Fig. 3C) were different to those of BL21 AI lipids when analyzed by TLC (Fig. 3B). At time points closer to 22 h, BL21 AI-MGS lipids had the tendency to migrate closer to the solvent front (indicated with ⇐) in contrast to BL21 AI lipids, which preferred to migrate closer to the application spot (indicated with App.). This observation suggested that there might be different types of modifications present in BL21 AI and BL21 AI-MGS lipids. The time-dependent differences in the migration profile of BL21 AI-MGS lipids were most prominent for phosphatidylethanolamine (PE). A very small migration shift was also observed for phosphatidylglycerol (PG) lipid. However, migration profiles for cardiolipin (CL) and α-glucosyldiacylglycerol (GlcDAG), the enzymatic product of MGS, remained almost unaffected.

3.3. Fatty acid composition in MGS-overexpressing cells

To better understand changes occurring in the lipid bilayer, fatty acid methyl esters (FAMEs) of purified PE lipid and total lipid extracts were both analyzed by gas chromatography (Fig. 4 and Figure S4, Supporting Information). Although MGS-expressing cells should be similar to control cells at the 0 h point, the fatty acid content was slightly different due to leaky expression of MGS (Table 2). The data shown in Table 2 indicate that cyclopropanated fatty acid content was greatly increased in BL21 AI cells after 22 h and constituted 30.8% of PE lipid and 23.2% of all lipids (total extract) at the stationary phase. However, BL21 AI-MGS membranes showed a different behavior where percentages of cyclopropanated species ($17{:}\Delta^{9,10}$ and $19{:}\Delta^{9,10}$) did not increase to

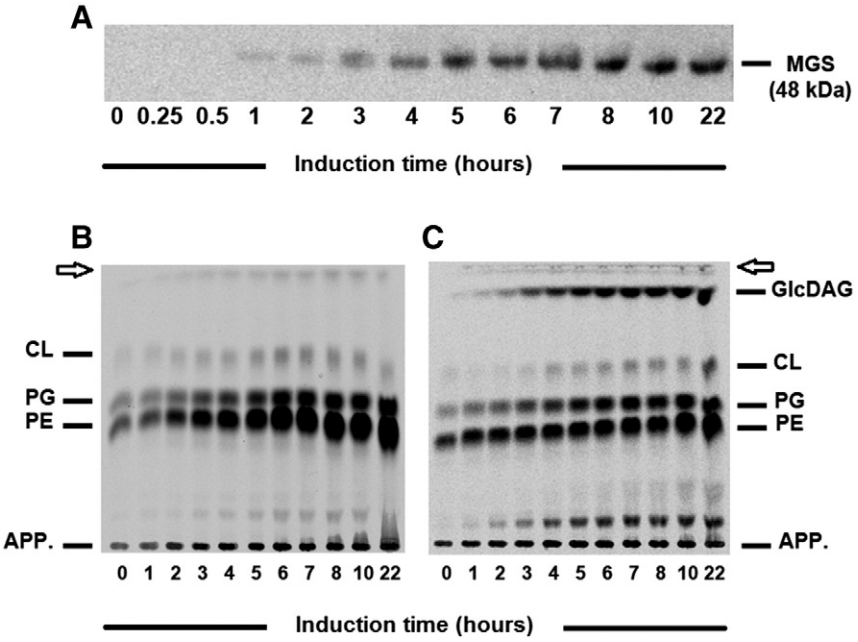

Fig. 3. Time dependent protein (MGS) and lipid production. (A) Western blot of BL21 AI-MGS cells with increasing MGS quantities, (B) Thin layer chromatograms of lipids extracted from BL21 AI cells and (C) BL21 AI-MGS cells. App. indicates the application spot and the linear solvent front (indicated with arrows) should be taken into consideration for both plates. * represents an unknown lipid which is believed to be a lyso-species of PE lipid.

the same level (4.9% for PE and 3.5% for total extract) as was observed in BL21 AI membranes (28.0% for PE and 23.2% for total extract) (Table 2). Furthermore, MGS-producing cells had higher unsaturation levels (more double bonds) (56.6% unsaturated fatty acids for PE and 61.2% for total extract) at the end of the induction process in comparison with BL21 AI cells (30.8% for PE and 36.4% for total extract). Comparison of the origin (0 h) and termination points (22 h) of induction had shown that unsaturation levels remained almost constant in BL21 AI-MGS membranes (initially 62.3%, after 22 h to 61.2%, total extract) while BL21 AI membranes had a dramatic decrease in double bond content (initially 61.3% to 36.4%, total extract) (Table 2). At 22 h, this 24.9% decrease in double bond content was followed by a 23.2% increase in cyclopropanated fatty acid content. Taken together, the data indicate reduced cyclopropanation of fatty acids in BL21 AI-MGS membranes.

3.4. Role of MGS protein on stress regulation and CFA synthase activity

To better understand the reduced cyclopropanation in MGS-expressing cells, we monitored the transcription of the *cfa* gene, which encodes for the CFA synthase. CFA synthase was selected because it is the only enzyme that cyclopropanates fatty acids in *E. coli*. A sharp increase in *cfa* transcription was observed in BL21 AI cells during 22 h (Fig. 5, left), in good agreement with results obtained with gas chromatography (Fig. 4 and Figure S4, Supporting Information). 6 h after induction, *cfa* transcription in BL21 AI cells had increased 4-fold and continued to increase until a 7-fold increase of the initial transcription was obtained at 22 h. No such trend was observed in BL21 AI-MGS cells, where promoter activity remained more or the less at a constant level for the first 6 h after induction. This was followed by a slight increase in *cfa* transcription (only 3-fold of the initial activity) at 22 h of induction (Fig. 5, right).

Transcription rates of other genes (*rpoE rseABC*, *plsB* and *psd*) involved in cell envelope metabolism [9,49–52], were also measured. RpoE is the final protein product of σ^E-dependent cell envelope stress response [53]. PlsB is the first enzyme that transfers a fatty acid chain to glycerol-3-phosphate (G3P) backbone [54] and PSD enzyme is responsible for the formation of PE lipid from the decarboxylation of phosphatidylserine [55]. Transcription levels of *rpoE*, *plsB* and *psd* genes were very similar in both cells.

Table 1
Lipid/protein ratios at different stages of induction are given as weight/weight ratios according to the calibration curve (Figure S3, Supporting Information).

	Samples	Amide I (cm^{-1}) (proteins)	C=O (cm^{-1}) (lipids)	Lipid/protein ratio (w/w)
BL21 AI	0 h	22.76 ± 0.2	0.72 ± 0.03	0.032 ± 0.001
	6 h	25.50 ± 0.3	0.84 ± 0.01	0.033 ± 0.002
	22 h	27.00 ± 0.1	0.78 ± 0.01	0.029 ± 0.001
BL21 AI-MGS	0 h	24.87 ± 0.1	0.75 ± 0.015	0.030 ± 0.0015
	6 h	28.48 ± 0.15	1.03 ± 0.018	0.036 ± 0.0035
	22 h	29.93 ± 0.2	1.20 ± 0.023	0.040 ± 0.0028

3.5. Acyl chain ordering of lipids during MGS production

Besides screening the order of membranes during MGS overexpression via monitoring lipid/protein ratios, analysis of IR spectra taken at different time points during induction enabled us to evaluate the combined effect of changes in cyclopropanation and unsaturation levels on the acyl chain ordering of lipids.

Secondary derivatives of the spectra taken with intact cells indicated systematic changes during induction of the spectral position of the CH_2 stretching bands at 2850 and 2920 cm^{-1}. These bands shift towards higher wavenumbers during gel to liquid crystalline phase transitions and provide a sensitive measure for conformational flexibility of the lipids [56,57]. Fig. 6 shows band shifts towards higher wavenumbers at 2850 cm^{-1} (Fig. 6A) and at 2920 cm^{-1} (Fig. 6B), which was detected for both BL21 AI and BL21 AI-MGS cells. For both bands, the shift is larger for BL21 AI cells and the band position at 10 and 22 h (stationary phase) is similar for both cells. Before induction (at 0 h), BL21 AI and BL21 AI-MGS cells had different wavenumbers as starting points due to the leaky expression of MGS described previously in this work. The spectral shifts observed for two CH_2 stretching vibrations correspond to 20% of the shift observed for lipid phase transitions between the gel and the liquid-crystalline phase.

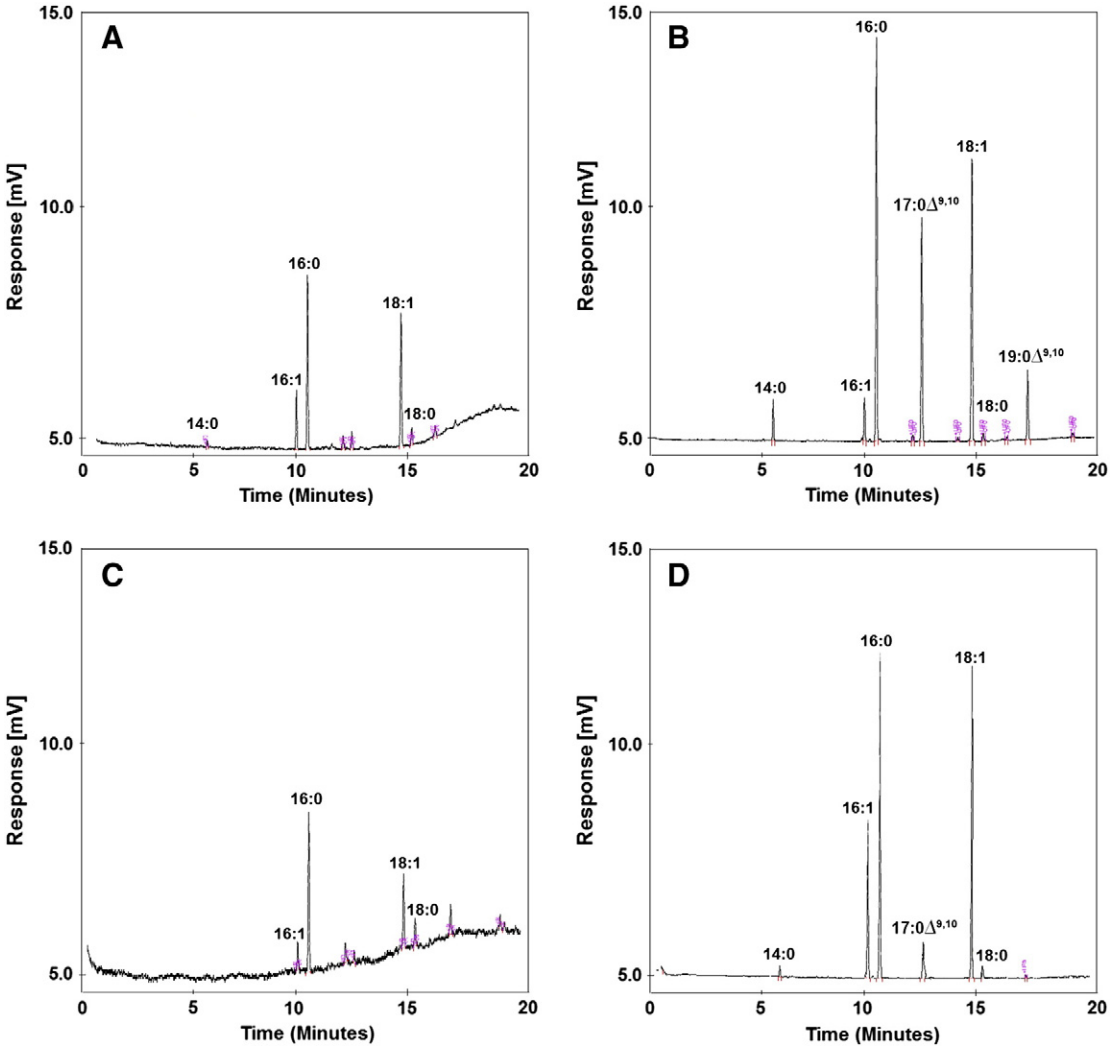

Fig. 4. GC chromatograms of PE lipid purified from (A) BL21 AI cells after 0 h, (B) 22 h of induction, (C) BL21 AI-MGS cells after 0 h and (D) after 22 h.

4. Discussion

Biological cells need to maintain a liquid-crystalline phase to achieve optimal cellular functions. This is usually achieved via fatty acid and/or headgroup modifications of the lipids, also referred to as *homoviscous adaptation* [15,58,59]. This work studied several parameters that are important for the *homoviscous adaptation* in *E. coli* during MGS overexpression. The parameters that were examined included the level of unsaturation and the extent of cyclopropanation of fatty acids. In addition to these parameters, the membrane ordering for intact cells, plasma membrane (inner and outer membranes; IM&OM) and intracellular vesicles of MGS-expressing cells was also monitored and compared with the findings obtained for BL21 AI control cells/membranes. We find that MGS-expressing cells and the control cells maintain a similar level of membrane order, but that they achieve this by different mechanisms. For the BL21 AI control cells, an almost unchanged lipid/protein ratio confirms that bacterial membranes are highly regulated even in the presence of IPTG. In contrast, MGS-expressing cells showed a distinctly different behavior and MGS protein was observed to create an imbalance in the lipid/protein ratio (Table 1). This imbalance was also observed for isolated membranes of MGS-expressing cells (Table S1, Supporting Information) in agreement with results in Table 1. However, no obvious difference in lipid/protein ratios was seen for plasma membrane and vesicle fractions of BL21 AI-MGS cells. An increased lipid/protein ratio, as seen in this work, has been associated with increased fluidity of lipids and reduced membrane order [12,26,29,60]. However, *E. coli* needs to maintain a certain degree of fluidity and membrane order, therefore it triggers regulative pathways [61]. One of the most common protective mechanisms is the diversification of lipid and fatty acid composition [7,61], and was found to be modified in an alternative way as seen in MGS-overexpressing cells.

The fatty acid pool in *E. coli* is normally a mixture of palmitate (16:0), palmitoleate (16:1) and cis-vaccenate (18:1) [62,63]. The unsaturated/saturated fatty acid ratio increases when cells are grown at low temperatures (22 °C, as in this work) [64] and a great amount of cyclopropanated species (methylene hexadecanoic and methylene octadecanoic acids: 17:0$\Delta^{9,10}$ and 19:0$\Delta^{9,10}$) were found to be produced at the expense of double bonds after cells enter stationary phase [65,66]. Our GC analyses of fatty acids from PE and total lipid extracts (Fig. 4 and Figure S4, Supporting Information, respectively) of BL21 AI cells substantiated this adaptation. In contrast, our data indicate that BL21 AI-MGS cells behave in a different way without significantly changing the level of unsaturation and of cyclopropanation.

Cyclopropanated fatty acids (CFAs) pack more poorly into an acyl-chain array than unsaturated fatty acids (UFAs). Thus a membrane with higher CFA/UFA ratio has a tendency to be in the liquid-crystalline phase (more fluid, less ordered) compared to the membranes with lower CFA/UFA ratios [66]. The higher unsaturation levels

Table 2
Fatty acid composition (%) of PE lipid (Table 2A) and total extract (Table 2B) from BL21 AI and BL21 AI-MGS cells. Each peak is integrated individually and % of individual peak is calculated considering all species detected in the sample. Triplicate measurements were performed for each sample and standard error was calculated. * corresponds to the remaining species found in the extract. [a], indicates fatty acids longer than 20:0 and [b], designates for fatty acids shorter than 14:0 (12:0 and 3 – OH 12:0 fatty acids with a ratio of 0.3% and 0.2% respectively).

A	BL21 AI 0 h	BL21 AI 22 h	BL21 AI-MGS 0 h	BL21 AI-MGS 22 h
14:0	1.3 ± 0.002	3.1 ± 0.001	–	1.1 ± 0.043
16:0	39.5 ± 0.041	36.3 ± 0.125	47.8 ± 0.196	35.9 ± 0.148
16:1	14.1 ± 0.023	3.8 ± 0.024	2.6 ± 0.164	18.6 ± 0.097
17:0	1.7 ± 0.029	0.3 ± 0.008	6.3 ± 0.028	–
17:0Δ^{9,10}	4.0 ± 0.015	21.5 ± 0.024	1.8 ± 0.066	4.4 ± 0.100
18:0	0.6 ± 0.019	0.6 ± 0.029	6.2 ± 0.012	1.6 ± 0.056
18:1	33.7 ± 0.085	27.0 ± 0.347	16.3 ± 0.074	38.0 ± 0.199
19:0Δ^{9,10}	–	6.5 ± 0.184	–	0.5 ± 0.023
*	5.1[a] ± 0.120	0.9[a] ± 0.098	19.0[a] ± 0.124	–[a]
B	**BL21 AI 0 h**	**BL21 AI 22 h**	**BL21 AI-MGS 0 h**	**BL21 AI-MGS 22 h**
14:0	2.8 ± 0.029	3.7 ± 0.075	1.6 ± 0.048	1.5 ± 0.052
16:0	29.7 ± 0.098	35.7 ± 0.084	30.4 ± 0.052	32.3 ± 0.094
16:1	18.3 ± 0.129	5.2 ± 0.052	18.7 ± 0.083	19.2 ± 0.214
17:0	–	0.8 ± 0.009	–	–
17:0Δ^{9,10}	3.8 ± 0.100	17.3 ± 0.086	4.4 ± 0.044	3.0 ± 0.084
18:0	1.3 ± 0.035	0.4 ± 0.012	0.2 ± 0.002	0.8 ± 0.007
18:1	43.0 ± 0.087	31.2 ± 0.051	43.6 ± 0.154	42.0 ± 0.129
19:0Δ^{9,10}	1.1 ± 0.075	5.9 ± 0.150	1.3 ± 0.032	0.5 ± 0.050
*	–[b]	–[b]	–[b]	0.7[b] ± 0.052

and decreased cyclopropanation levels (Table 2) shift BL21 AI-MGS membranes to a more ordered state compared to BL21 AI cell membranes. This seems to be a protective adaptation to prevent membrane disorder caused by the increased lipid/protein ratio. According to the similar spectral position of the infrared absorption of the CH_2 stretching bands in Fig. 6, the overall effect of these changes results in a similar membrane state for BL21 AI and BL21 AI-MGS membranes.

The decreased cyclopropanation of fatty acids was also confirmed at a transcriptional level, with lowered promoter activity of the gene encoding cyclopropane fatty acid synthase (CFA), an enzyme responsible for the cyclopropanation of unsaturated fatty acids (UFA) (Fig. 5). CFA [66,67] and MGS [40,41,68] are both membrane associated and dependent on specific charge interactions with anionic lipids in order to be active. Reduced transcription of *cfa* indicates a metabolic regulation against a fatal imbalance of fluidity and the membrane order but also points at the possibility of a potential MGS-CFA competition (Fig. 7). Since both enzymes are binding to anionic lipids in the membrane, an excessive amount of MGS produced in the cell can result in CFA synthase to be precluded from membrane binding. The present work is the first

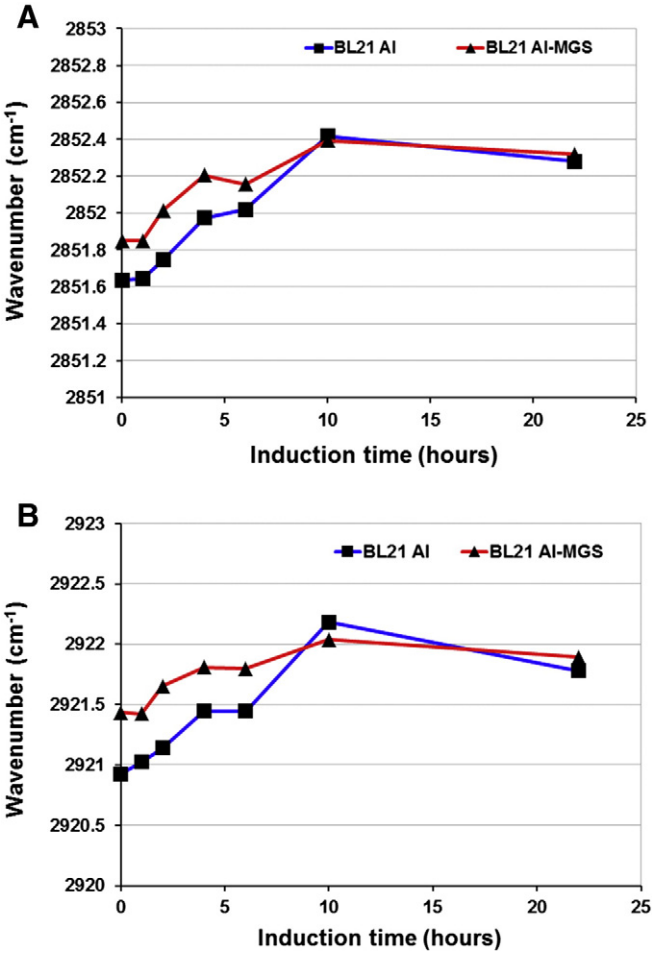

Fig. 6. Acyl chain ordering in BL21 AI (■) and BL21 AI-MGS cells (▲). Frequency shifts for (A) CH_2 symmetric stretch, (B) CH_2 asymmetric stretch vibrations. Each band position was determined for two independent set of experiments and the averaged band positions of both experimental data sets were plotted.

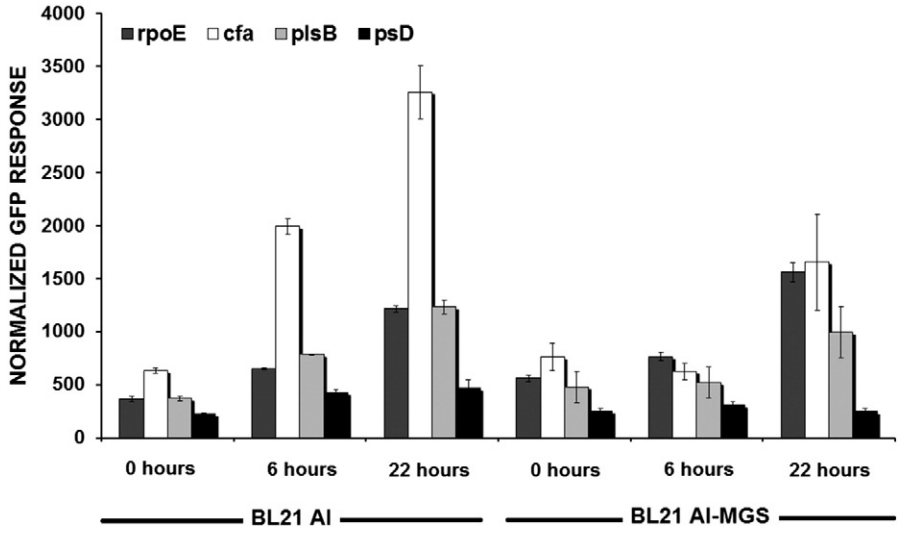

Fig. 5. Transcriptional activities of promoter regions (*cfa*, *rpoE*, *plsB* and *psd*) fused to *gfp*. Whole cell fluorescence was normalized against the OD_{600} values.

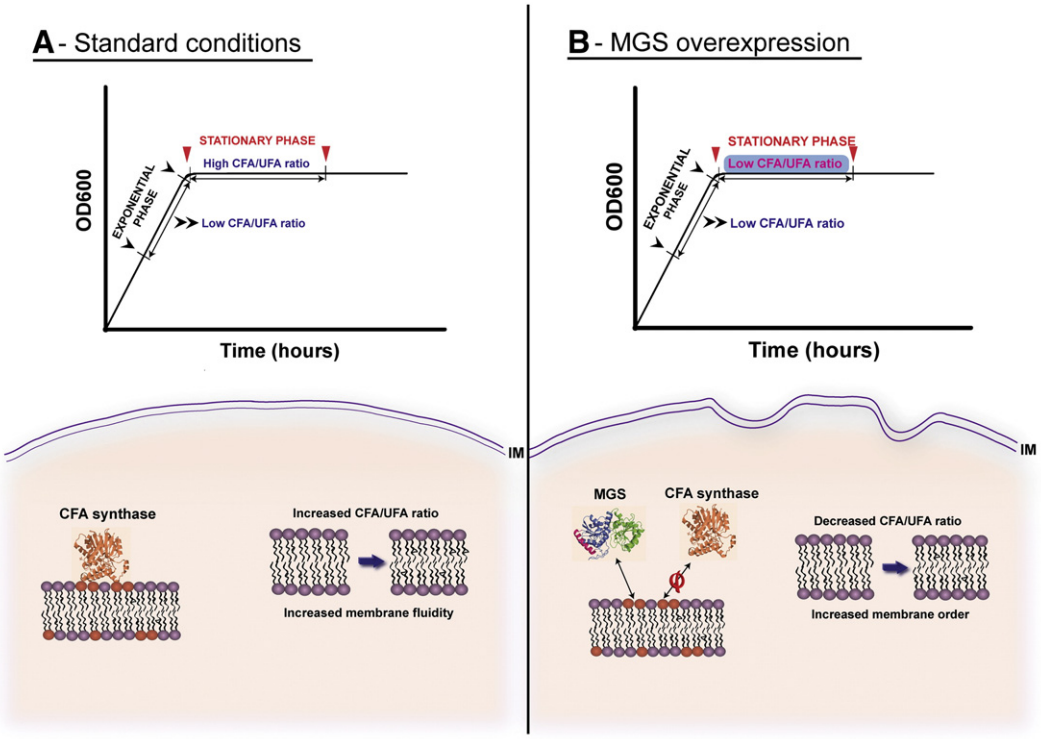

Fig. 7. Schematic presentation of fatty acid modeling in *E. coli* cells (A) under standard growth conditions and (B) MGS overexpression. MGS is represented here with a prediction model (No available x-ray structure) [39,40]. Since *E. coli* CFA synthase x-ray structure is unsolved, CFA synthase was presented with the x-ray structure from *Mycobacterium Tuberculosis* (PDB ID: 1KGP). Red and purple colored lipid headgroups represent anionic phospholipids (PG and CL) and zwitterionic phospholipids (PE), respectively.

study to reveal a relationship between overexpression of MGS protein and reduced cyclopropanation of fatty acids (Fig. 7). The reported modification serves to preserve similar membrane state as in control cells, in spite of the higher lipid/protein ratio in the MGS expressing cells. This, in turn, likely helps the cell to maintain a certain membrane state when accommodating large quantities of the MGS protein. The actual mechanism(s) leading to vesiculation still remain to be elucidated. However, the current data and insights concerning the ability of MGS to remodel *E. coli* membranes should also be taken into consideration in further investigations on the vesiculation mechanisms of MGS and other vesiculating proteins.

Dedication

We would like to commemorate this work to Prof. Åke Wieslander who passed away in March, 2013. We will always remember him as a great personality, devoted scientist and good spirited friend.

Funding

This research was supported by funds from Swedish Foundation for Strategic Research (SSF), Vetenskapsrådet (Project no: 621-2006-4818; 2008-19122-62107-3 and 621-2011-3524) and Knut and Alice Wallenbergs Stiftelse, Sweden. Ljubica Lindholm acknowledges a Carl Tryggers Foundation post-doctoral stipend.

Acknowledgements

The authors would also like to thank Carin Larsson for technical assistance with GC-MS measurements, Dr. Changrong Ge for scientific discussions and Dr. Hanna Eriksson for preparation of BL21 AI-MGS clone.

Appendix A. Supplementary data

Supplementary data to this article can be found online at http://dx.doi.org/10.1016/j.bbamem.2014.04.001.

References

[1] N.P. Barrera, M. Zhou, C.V. Robinson, The role of lipids in defining membrane protein interactions: insights from mass spectrometry, Trends Cell Biol. 23 (2013) 1–8.
[2] D.C. Mitchell, Progress in understanding the role of lipids in membrane protein folding, Biochim. Biophys. Acta 1818 (2012) 951–956.
[3] R. Phillips, T. Ursell, P. Wiggins, P. Sens, Emerging roles for lipids in shaping membrane-protein function, Nature 459 (2009) 379–385.
[4] R. Schneiter, A. Toulmay, The role of lipids in the biogenesis of integral membrane proteins, Appl. Microbiol. Biotechnol. 73 (2007) 1224–1232.
[5] C.R. Woese, Bacterial evolution, Microbiol. Rev. 51 (1987) 221–271.
[6] Y.L. Yang, F.L. Yang, S.C. Jao, M.Y. Chen, S.S. Tsay, W. Zou, S.H. Wu, Structural elucidation of phosphoglycolipids from strains of the bacterial thermophiles *Thermus* and *Meiothermus*, J. Lipid Res. 47 (2006) 1823–1832.
[7] Y.M. Zhang, C.O. Rock, Membrane lipid homeostasis in bacteria, Nat. Rev. Microbiol. 6 (2008) 222–233.
[8] Y.M. Zhang, C.O. Rock, A rainbow coalition of lipid transcriptional regulators, Mol. Microbiol. 78 (2010) 5–8.
[9] J.B. Parsons, C.O. Rock, Bacterial lipids: metabolism and membrane homeostasis, Prog. Lipid Res. 52 (2013) 249–276.
[10] M. Sinensky, Homeoviscous adaptation-a homeostatic process that regulates the viscosity of membrane lipids in *Escherichia coli*, Proc. Natl. Acad. Sci. U. S. A. 71 (1974) 522–525.
[11] Y. Yano, A. Nakayama, K. Ishihara, H. Saito, Adaptive changes in membrane lipids of Barophilic bacteria in response to changes in growth pressure, Appl. Environ. Microbiol. 64 (1998) 479–485.
[12] P.M. Oger, A. Cario, Adaptation of the membrane in archaea, Biophys. Chem. 183 (2013) 42–56.
[13] Y.H. Itoh, A. Sugai, I. Uda, T. Itoh, The evolution of lipids, Adv. Space Res. 28 (2001) 719–724.
[14] Y. Koga, Thermal adaptation of the archaeal and bacterial lipid membranes, Archaea 2012 (2012) 789652.
[15] A. Alvarez-Ordonez, A. Fernandez, M. Lopez, A. Bernardo, Relationship between membrane fatty acid composition and heat resistance of acid and cold stressed *Salmonella senftenberg* CECT 4384, Food Microbiol. 26 (2009) 347–353.

[16] J.E. Cronan Jr., Phospholipid modifications in bacteria, Curr. Opin. Microbiol. 5 (2002) 202–205.
[17] L. Shabala, T. Ross, Cyclopropane fatty acids improve *Escherichia coli* survival in acidified minimal media by reducing membrane permeability to H^+ and enhanced ability to extrude H^+, Res. Microbiol. 159 (2008) 458–461.
[18] S. Lee, Y. Jung, S. Lee, J. Lee, Correlations between FAS elongation cycle genes expression and fatty acid production for improvement of long-chain fatty acids in *Escherichia coli*, Appl. Biochem. Biotechnol. 169 (2013) 1606–1619.
[19] Y.M. Zhang, H. Marrakchi, C.O. Rock, The FabR (YijC) transcription factor regulates unsaturated fatty acid biosynthesis in *Escherichia coli*, J. Biol. Chem. 277 (2002) 15558–15565.
[20] Y. Fujita, H. Matsuoka, K. Hirooka, Regulation of fatty acid metabolism in bacteria, Mol. Microbiol. 66 (2007) 829–839.
[21] C. Suarez-Germa, M.T. Montero, J. Ignes-Mullol, J. Hernandez-Borrell, O. Domenech, Acyl chain differences in phosphatidylethanolamine determine domain formation and LacY distribution in biomimetic model membranes, J. Phys. Chem. B 115 (2011) 12778–12784.
[22] Z. Yao, R.M. Davis, R. Kishony, D. Kahne, N. Ruiz, Regulation of cell size in response to nutrient availability by fatty acid biosynthesis in *Escherichia coli*, Proc. Natl. Acad. Sci. U. S. A. 109 (2012) E2561–E2568.
[23] Y. Cao, J. Yang, M. Xian, X. Xu, W. Liu, Increasing unsaturated fatty acid contents in *Escherichia coli* by coexpression of three different genes, Appl. Microbiol. Biotechnol. 87 (2010) 271–280.
[24] C.O. Rock, J.T. Tsay, R. Heath, S. Jackowski, Increased unsaturated fatty acid production associated with a suppressor of the fabA6(Ts) mutation in *Escherichia coli*, J. Bacteriol. 178 (1996) 5382–5387.
[25] R. Sugai, H. Shimizu, K. Nishiyama, H. Tokuda, Overexpression of yccL (gnsA) and ydfY (gnsB) increases levels of unsaturated fatty acids and suppresses both the temperature-sensitive fabA6 mutation and cold-sensitive secG null mutation of *Escherichia coli*, J. Bacteriol. 183 (2001) 5523–5528.
[26] J.S. Owen, K.R. Bruckdorfer, R.C. Day, N. McIntyre, Decreased erythrocyte membrane fluidity and altered lipid composition in human liver disease, J. Lipid Res. 23 (1982) 124–132.
[27] M.C. Mansilla, L.E. Cybulski, D. Albanesi, D. deMendoza, Control of membrane lipid fluidity by molecular thermosensors, J. Bacteriol. 186 (2004) 6681–6688.
[28] G. Lenaz, Lipid fluidity and membrane protein dynamics, Biosci. Rep. 7 (1987) 823–837.
[29] S. Huffer, M.E. Clark, J.C. Ning, H.W. Blanch, D.S. Clark, Role of alcohols in growth, lipid composition, and membrane fluidity of yeasts, bacteria and archaea, Appl. Environ. Microbiol. 77 (2011) 6400–6408.
[30] F. Gubellini, G. Verdon, N.K. Karpowich, J.D. Luff, G. Boel, N. Gauthier, S.K. Handelman, S.E. Ades, J.F. Hunt, Physiological response to membrane protein overexpression in *E. coli*, Mol. Cell. Proteomics 10 (2011) (M111 007930).
[31] S. Wagner, L. Baars, A.J. Ytterberg, A. Klussmeier, C.S. Wagner, O. Nord, P.A. Nygren, K.J. van Wijk, J.W. de Gier, Consequences of membrane protein overexpression in *Escherichia coli*, Mol. Cell. Proteomics 6 (2007) 1527–1550.
[32] I. Arechaga, B. Miroux, S. Karrasch, R. Huijbregts, B. de Kruijff, M.J. Runswick, J.E. Walker, Characterisation of new intracellular membranes in *Escherichia coli* accompanying large scale over-production of the b subunit of F(1)F(o) ATP synthase, FEBS Lett. 482 (2000) 215–219.
[33] C.E. Carty, L.O. Ingram, Lipid synthesis during the *Escherichia coli* cell cycle, J. Bacteriol. 145 (1981) 472–478.
[34] M.P. Gent, P.F. Cottam, C. Ho, A biophysical study of protein–lipid interactions in membranes of *Escherichia coli*. Fluoromyristic acid as a probe, Biophys. J. 33 (1981) 211–223.
[35] E. van den Brink-van der Laan, J.W. Boots, R.E. Spelbrink, G.M. Kool, E. Breukink, J.A. Killian, B. de Kruijff, Membrane interaction of the glycosyltransferase MurG: a special role for cardiolipin, J. Bacteriol. 185 (2003) 3773–3779.
[36] L.E. Metzger, C.R. Raetz, Purification and characterization of the lipid A disaccharide synthase (LpxB) from *Escherichia coli*, a peripheral membrane protein, Biochemistry 48 (2009) 11559–11571.
[37] J.H. Weiner, B.D. Lemire, M.L. Elmes, R.D. Bradley, D.G. Scraba, Overproduction of fumarate reductase in *Escherichia coli* induces a novel intracellular lipid–protein organelle, J. Bacteriol. 158 (1984) 590–596.
[38] M.L. Elmes, D.G. Scraba, J.H. Weiner, Isolation and characterization of the tubular organelles induced by fumarate reductase overproduction in *Escherichia coli*, J. Gen. Microbiol. 132 (1986) 1429–1439.
[39] H.M. Eriksson, P. Wessman, C. Ge, K. Edwards, A. Wieslander, Massive formation of intracellular membrane vesicles in *Escherichia coli* by a monotopic membrane-bound lipid glycosyltransferase, J. Biol. Chem. 284 (2009) 33904–33914.
[40] C. Arioz, W. Ye, A. Bakali, C. Ge, J. Liebau, H. Gotzke, A. Barth, A. Wieslander, L. Maler, Anionic lipid binding to the foreign protein MGS provides a tight coupling between phospholipid synthesis and protein overexpression in *Escherichia coli*, Biochemistry 52 (2013) 5533–5544.
[41] J. Lind, T. Ramo, M.L. Klement, E. Barany-Wallje, R.M. Epand, R.F. Epand, L. Maler, A. Wieslander, High cationic charge and bilayer interface-binding helices in a regulatory lipid glycosyltransferase, Biochemistry 46 (2007) 5664–5677.
[42] L. Li, P. Storm, O.P. Karlsson, S. Berg, A. Wieslander, Irreversible binding and activity control of the 1,2-diacylglycerol 3-glucosyltransferase from *Acholeplasma laidlawii* at an anionic lipid bilayer surface, Biochemistry 42 (2003) 9677–9686.
[43] M. Almgren, K. Edwards, G. Karlsson, Cryo transmission electron microscopy of liposomes and related structures, Colloids Surf. A 174 (2000) 3–21.
[44] E.G. Bligh, W.J. Dyer, A rapid method of total lipid extraction and purification, Can. J. Biochem. Physiol. 37 (1959) 911–917.
[45] E. Goormaghtigh, V. Raussens, J.M. Ruysschaert, Attenuated total reflection infrared spectroscopy of proteins and lipids in biological membranes, Biochim. Biophys. Acta 1422 (1999) 105–185.
[46] A.A. Spector, M.A. Yorek, Membrane lipid composition and cellular function, J. Lipid Res. 26 (1985) 1015–1035.
[47] A. Mrozik, Z. Piotrowska-Seget, S. Labuzek, Cytoplasmic bacterial membrane responses to environmental perturbations, Pol. J. Environ. Stud. 13 (2004) 487–494.
[48] P. North, S. Fleischer, Alteration of synaptic membrane cholesterol/phospholipid ratio using a lipid transfer protein. Effect on gamma-aminobutyric acid uptake, J. Biol. Chem. 258 (1983) 1242–1253.
[49] Z. Yao, R.M. Davis, R. Kishony, D. Kahne, N. Ruiz, Regulation of cell size in response to nutrient availability by fatty acid biosynthesis in *Escherichia coli*, Proc. Natl. Acad. Sci. U. S. A. 109 (2013) E2561–E2568.
[50] L. Paoletti, Y.J. Lu, G.E. Schujman, D. de Mendoza, C.O. Rock, Coupling of fatty acid and phospholipid synthesis in *Bacillus subtilis*, J. Bacteriol. 189 (2007) 5816–5824.
[51] Y.Y. Chang, J. Eichel, J.E. Cronan Jr., Metabolic instability of *Escherichia coli* cyclopropane fatty acid synthase is due to RpoH-dependent proteolysis, J. Bacteriol. 182 (2000) 4288–4294.
[52] C.L. Cooper, S. Jackowski, C.O. Rock, Fatty acid metabolism in sn-glycerol-3-phosphate acyltransferase (plsB) mutants, J. Bacteriol. 169 (1987) 605–611.
[53] J.D. Hayden, S.E. Ades, The extracytoplasmic stress factor, sigmaE, is required to maintain cell envelope integrity in *Escherichia coli*, PLoS One 3 (2008) e1573.
[54] A. Wahl, L. My, R. Dumoulin, J.N. Sturgis, E. Bouveret, Antagonistic regulation of dgkA and plsB genes of phospholipid synthesis by multiple stress responses in *Escherichia coli*, Mol. Microbiol. 80 (2011) 1260–1275.
[55] Q.X. Li, W. Dowhan, Structural characterization of *Escherichia coli* phosphatidylserine decarboxylase, J. Biol. Chem. 263 (1988) 11516–11522.
[56] N. Loffhagen, C. Härtig, W. Geyer, M. Voyevoda, H. Harms, Competition between cis, trans and cyclopropane fatty acid formation and its impact on membrane fluidity, Eng. Life Sci. 7 (2007) 67–74.
[57] D.J. Moore, M. Wyrwa, C.P. Reboulleau, R. Mendelsohn, Quantitative IR studies of acyl chain conformational order in fatty acid homogeneous membranes of live cells of *Acholeplasma laidlawii* B, Biochemistry 32 (1993) 6281–6287.
[58] M.C. Mansilla, L.E. Cybulski, D. Albanesi, D. de Mendoza, Control of membrane lipid fluidity by molecular thermosensors, J. Bacteriol. 186 (2004) 6681–6688.
[59] T. Toyoda, Y. Hiramatsu, T. Sasaki, Y. Nakaoka, Thermo-sensitive response based on the membrane fluidity adaptation in *Paramecium multimicronucleatum*, J. Exp. Biol. 212 (2009) 2767–2772.
[60] T.A. Brasitus, R.S. Keresztes, Isolation and partial characterization of basolateral membranes from rat proximal colonic epithelial cells, Biochim. Biophys. Acta 728 (1983) 11–19.
[61] D. de Mendoza, A. Klages Ulrich, J.E. Cronan Jr., Thermal regulation of membrane fluidity in *Escherichia coli*. Effects of overproduction of beta-ketoacyl-acyl carrier protein synthase I, J. Biol. Chem. 258 (1983) 2098–2101.
[62] K. Magnuson, S. Jackowski, C.O. Rock, J.E. Cronan Jr., Regulation of fatty acid biosynthesis in *Escherichia coli*, Microbiol. Rev. 57 (1993) 522–542.
[63] C.R. Raetz, Enzymology, genetics, and regulation of membrane phospholipid synthesis in *Escherichia coli*, Microbiol. Rev. 42 (1978) 614–659.
[64] A.G. Marr, J.L. Ingraham, Effect of temperature on the composition of fatty acids in *Escherichia coli*, J. Bacteriol. 84 (1962) 1260–1267.
[65] M.A. Casadei, P. Manas, G. Niven, E. Needs, B.M. Mackey, Role of membrane fluidity in pressure resistance of *Escherichia coli* NCTC 8164, Appl. Environ. Microbiol. 68 (2002) 5965–5972.
[66] D.W. Grogan, J.E. Cronan Jr., Cyclopropane ring formation in membrane lipids of bacteria, Microbiol. Mol. Biol. Rev. 61 (1997) 429–441.
[67] F.R. Taylor, J.E. Cronan Jr., Cyclopropane fatty acid synthase of *Escherichia coli*. Stabilization, purification, and interaction with phospholipid vesicles, Biochemistry 18 (1979) 3292–3300.
[68] M. Edman, S. Berg, P. Storm, M. Wikstrom, S. Vikstrom, A. Ohman, A. Wieslander, Structural features of glycosyltransferases synthesizing major bilayer and nonbilayer-prone membrane lipids in *Acholeplasma laidlawii* and *Streptococcus pneumoniae*, J. Biol. Chem. 278 (2003) 8420–8428.